Concurrent shear stress and chemical stimulation of mechano-sensitive cells by discontinuous dielectrophoresis

Rebecca Soffe,[1,a)] Sara Baratchi,[2] Shi-Yang Tang,[1] Arnan Mitchell,[1] Peter McIntyre,[2] and Khashayar Khoshmanesh[1,a)]
[1]*School of Engineering, RMIT University, Victoria 3001, Australia*
[2]*School of Medical and Biomedical Science, RMIT University, Victoria 3083, Australia*

(Received 8 February 2016; accepted 17 March 2016; published online 4 April 2016)

Microfluidic platforms enable a variety of physical or chemical stimulation of single or multiple cells to be examined and monitored in real-time. To date, intracellular calcium signalling research is, however, predominantly focused on observing the response of cells to a single mode of stimulation; consequently, the sensitising/desensitising of cell responses under concurrent stimuli is not well studied. In this paper, we provide an extended Discontinuous Dielectrophoresis procedure to investigate the sensitising of chemical stimulation, over an extensive range of shear stress, up to 63 dyn/cm^2, which encompasses shear stresses experienced in the arterial and venus systems (10 to 60 dyn/cm^2). Furthermore, the TRPV4-selective agonist GSK1016790A, a form of chemical stimulation, did not influence the ability of the cells' to remain immobilised under high levels of shear stress; thus, enabling us to investigate shear stress stimulation on agonism. Our experiments revealed that shear stress sensitises GSK1016790A-evoked intracellular calcium signalling of cells in a shear-stimulus dependent manner, as observed through a reduction in the cellular response time and an increase in the pharmacological efficacy. Consequently, suggesting that the role of TRPV4 may be underestimated in endothelial cells—which experience high levels of shear stress. This study highlights the importance of conducting studies at high levels of shear stress. Additionally, our approach will be valuable for examining the effect of high levels of shear on different cell types under different conditions, as presented here for agonist activation. © *2016 AIP Publishing LLC*.
[http://dx.doi.org/10.1063/1.4945309]

INTRODUCTION

Calcium ion (Ca^{2+}) is a potent and versatile intracellular messenger that regulates a wide range of spatial and temporal cellular signals. Intracellular calcium level ($[Ca^{2+}]_i$) is tightly controlled by efflux from the cell through ion transporters, sequestration in intracellular compartments, buffering high affinity cytosolic calcium binding proteins, and influx through regulated ion channels.[1] Opening of calcium permeable channels in response to their selective stimulus, such as mechanical stress or agonists, causes an influx of Ca^{2+} into cells. This event increases the $[Ca^{2+}]_i$, which can be measured using Ca^{2+} sensitive dyes.

Microfluidic platforms have been widely used for various cell-based assays, including cell culturing, separation, analytic detection, and biochemical analysis, to name a few.[2–21] In the area of physiology, for example, signalling within and between cells, including calcium signalling, has been investigated using microfluidic based platforms.[22–26] In the event of designing a microfluidic platform to investigate intracellular calcium signalling of cells in suspension,

[a)]Electronic addresses: s3418162@student.rmit.edu.au and khashayar.khoshmanesh@rmit.edu.au

 © 2016 AIP Publishing LLC

several aspects need to be considered. For example, the immobilisation strategy used to immobilise cells to enable real-time observations, target cell population size, and the intended stimuli to be applied.

Commonly reported immobilisation approaches used for investigating intracellular calcium signalling on microfluidic platform include hydrodynamic trapping and surface modification.[9,24,27–32] In previously reported hydrodynamic trapping microfluidic platforms, different target cell populations have been investigated, from a single isolated cell to arrays of cells; in each case, the cells are trapped using various types of hydrodynamic "docks," which enables label free, high-throughput imaging of cells.[27,28,33,34] These hydrodynamic devices have enabled various stimuli to be investigated, including electric field excitation, thermal, chemical (commonly achieved through using specific inhibitors and activators), and physical stimuli (such as flow-induced shear stress or mechanical deformation, achieved by using various hydrodynamic structures).[23,24,27,28,33,34] For example, Xu *et al.* designed a microfluidic platform to isolate an individual HL60 cell from suspension, then in turn applying whole cell compression through a deflectable membrane, which resulted in Ca^{2+} flow through ion channels.[34] However, the use of hydrodynamic structures introduces the possible trapping of debris and limits shear stress investigation due to the influence of surrounding microstructures on shear stress profiles.

On the other hand, surface modification approaches use specific chemicals to coat the substrate surface, such as biomimetic peptides (for example, poly-(L-lysine) and poly-(L-ornithine)) or extracellular matrix proteins (for example, laminin and fibronectin).[2,30–32,35,36] Baratchi *et al.* investigated the influence of shear and thermal stresses, using a chemically modified substrate surface microfluidic platform. The platform incorporated a microchannel with contracting-expanding geometry, so that immobilised cells throughout the platform experienced different levels of shear stress. Additionally, thermal investigation was conducted by changing the temperature surrounding the microfluidic platform.[32] The cells immobilised using surface modification approaches become readily dislodged with increasing shear stress; consequently, shear stress investigations are limited to 20 dyn/cm^2.[32,37]

In summary, these aforementioned platforms, both hydrodynamic- and surface modified-microfluidic platforms, have provided insights into the intracellular calcium signalling responses of different cells. Such insights include metabolic monitoring; response to cardio-tonic agents and cardio-toxic chemotherapeutic for drug discovery; channel response to specific inhibitors and activators; and ion responses to a specific stimulus, such as shear stress or whole cell compression.[24,27,28,32–34,38] However, to date platforms have not been designed specifically to investigate high levels of shear stress on loosely adherent cells or to concurrently examine its effect on agonism of mechanically sensitive ion channels. To address this, we have extended our recently reported discontinuous dielectrophoresis approach to examine the effect of mechanical stimulation on agonist activation in HEK-293-TRPV4 cells through measuring intracellular calcium levels.[39] Discontinuous dielectrophoresis reduces the electric field activation duration compared to conventional dielectrophoresis; additionally, experiments can be conducted in biocompatible high-conductivity buffers, such as HEPES buffered saline (HBS), which helps to maintain cell viability and function. Discontinuous dielectrophoresis enables high shear stress analysis of cells, that are normally grown in suspension, or, do not attach well to substrate surfaces. Experiments can be undertaken at shear stress levels comparable to those observed in arterial and venus systems (10 to 60 dyn/cm^2); the highest levels of shear experienced by cells *in vivo*.[39,40]

Discontinuous dielectrophoresis enabled us to investigate the shear-induced calcium signalling of HEK-293 cells, expressing TRPV4.[39] TRPV4 is a non-selective Ca^{2+} permeable cation channel, which responds to various stimuli, including shear stress and chemical stimulation. Most of the 28 mammalian transient receptor potential (TRP) channels in this family are non-selective cation channels, which are opened by a variety of stimuli. TRPV4 is a mechano-sensitive channel expressed in vascular endothelial cells; these cells experience shear stress from blood flow. TRPV4 is a polymodal receptor, which plays important roles in cellular processes such as mechano-, thermo-, and osmo-sensation.[41,42] Here, we have used discontinuous dielectrophoresis to investigate the influence of shear stress on TRPV4 responses to its selective

agonist GSK1016790A in HEK-293-TRPV4 cells. Additionally, we compared agonist-induced calcium signalling characteristics of HEK-293-TRPV4 cells in HEPES buffered saline and the low electrical conductivity (LEC) buffer (routinely used in conventional dielectrophoresis microfluidic systems).

MATERIALS AND METHODS

Cell preparation

HEK-293 T-REx (Life Sciences) cell lines stably expressing human TRPV4 were generated by growing the cells in tetracycline-free DMEM (Dulbecco's Modified Eagle's medium) media supplemented 10% FBS (Fetal bovine serum), blasticidin (5 μg/ml), and hygromycin (50 μg/ml).[43] To induce TRP channel expression, 0.1 μg/ml of tetracycline was applied into the cell buffer 12 h before each experiment. HEK-293 T-REx cells that were not transfected were used as a negative control.

Prior to experiments, the 20 μl loaded cells were diluted in 1000 μl in a LEC buffer (8.5% w/v sucrose and 0.3% dextrose in deionised water). During the dilution process, one had to be careful when diluting the cells to minimise the occurrence of pre-exposing the cells to shear stress.

The intracellular level was obtained through measuring the light intensity of cells stained with Fluo-4AM dye, as previously explained.[32] The viability of cells was verified at the completion of each experiment through examining the viability of cells on-chip using propidium iodide (PI) stain (10 μg/ml).

GSK1016790A preparation

GSK1016790A (Sigma-Aldrich), a selective and cell-permeable agonist of the TRPV4 ion channel, was dissolved in DMSO (Dimethyl sulfoxide) and then diluted in HBS to obtain the desired concentrations of 12.5 and 3.125 nM. HBS contained 140 mmol/l NaCl, 5 mmol/l KCl, 10 mmol/l HEPES, 11 mmol/l D-glucose, 1 mmol/l $MgCl_2$, 2 mmol/l $CaCl_2$, and 2 mmol/l probenecid, adjusted to pH = 7.4.[44]

Platform fabrication

The microelectrodes were fabricated using standard photolithography and etching techniques; additionally, the polydimethylsiloxane (PDMS) microfluidic channel was fabricated using replica molding techniques.[45] The design of the gold-on-chrome microelectrodes, and 500 × 80 μm (width by height) PDMS microchannel, is presented in more detail in the supplementary material S1.[46]

Data analysis

Fluorescent intensity was determined through analysing areas defined as regions of interest (ROIs) which encapsulated single cells, using in-built functions of NIS element viewer (Nikon Instruments). To quantify changes in $[Ca^{2+}]_i$, the average intensity of selected ROIs was measured, and the results are reported as the ratio of F_1/F_0. Activation was defined as an increase in the summed fluorescent signal from test groups that exceeded three standard deviations from the mean of the control. The results are presented as mean ± SEM (standard error of the mean), and P values of less than 0.05 were considered significant ($^*P < 0.05$, $^{**}P < 0.01$, and $^{***}P < 0.001$). For statistical analysis, student t test or ANOVA was performed using the Graph pad prism software.

Numerical simulations

Computational Fluid Dynamic techniques were used to calculate the flow-induced shear stress. The Reynolds number obtained for a flow rate of 120 μl/min (the highest flow rate used in our experiments) was determined to be less than 10, indicating that the flow was characteristically laminar. Additionally, the buffer medium was considered as a Newtonian liquid. The

Navier-Stokes equations were solved using ANSYS Fluent 6.3 software package (Canonsburg, PA, USA), and the pressure-velocity terms were coupled using the SIMPLE algorithm. The Second-Order Upwind Scheme was used for discretization of convection terms. The simulations were performed in three-dimensional, in the presence of immobilised cells, as further detailed in the *Shear stress simulation analysis* section. Boundary conditions used throughout the simulations, included an ambient pressure at the inlet and the application of desired flow rates at the outlet. Furthermore, the surface of glass substrate, microchannel, and immobilised cells were considered as rigid walls with no-slip boundary condition applied.

RESULTS AND DISCUSSION

Discontinuous dielectrophoresis, an approach for immobilising loosely adherent cells to withstand high shear stress, was recently developed by our group.[39] Using this method, we have investigated the impact of shear stress on agonist activation of intracellular calcium signalling in HEK-293-TRPV4 cells. Discontinuous dielectrophoresis is required to immobilise loosely adherent cells, such that they are not washed away in high shear stress—other methods are limited to low shear stresses (less than 20 dyn/cm^2) or have adverse effects on cell integrity.[32,37,39] In this paper, the magnitude of shear stress is expressed in dyn/cm^2, the preferred unit to express shear stress in the field of mechanobiology (1 dyn/cm^2 = 0.1 N/m^2 = 0.1 Pa). In summary, discontinuous dielectrophoresis (Figure 1(a)) is a procedure undertaken on a microfluidic platform, described as follows (see supplementary material S1 for device design).[46] The cells were added to the microfluidic platform at a flow rate of 2.5 μl/min. Once the cells reached the microelectrodes, an electric field was used to immobilise them along the

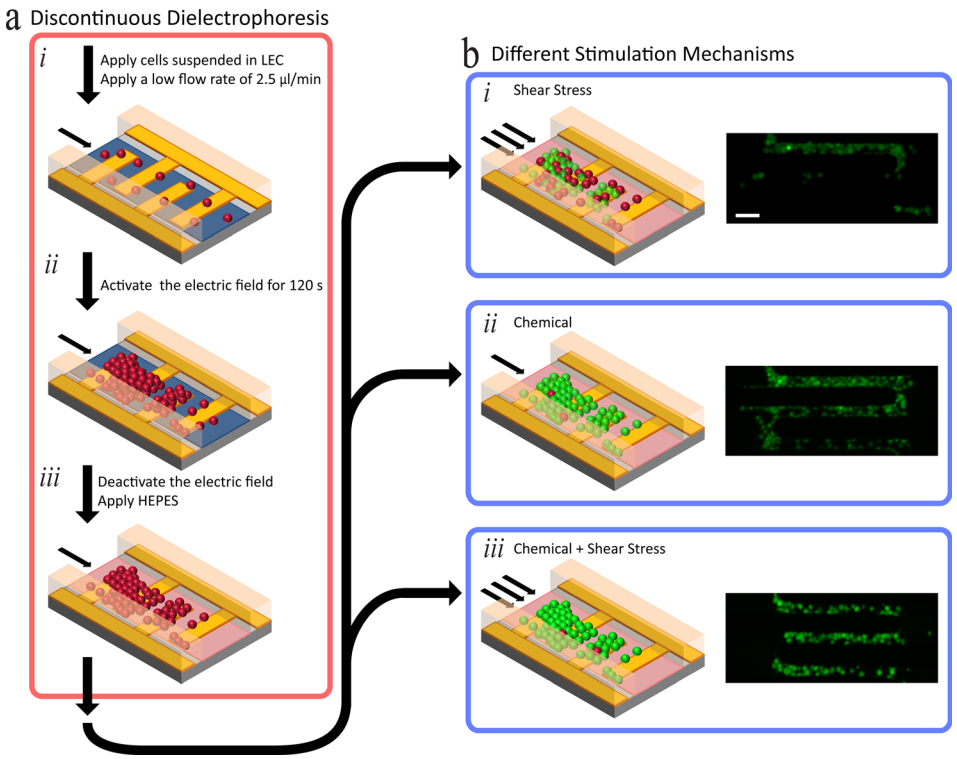

FIG. 1. Procedure for investigating intracellular calcium signalling of cells using different stimulation mechanisms. (a) Discontinuous dielectrophoresis process, image adapted from our recently published work entailing the complete discontinuous dielectrophoresis procedure.[39] (b) Stimulation of immobilised cells using different mechanisms: (i) Investigating chemical induced calcium signalling, achieved by applying agonists such as GSK1016790A, at a low flow rate of 2.5 μl/min. (ii) Investigating shear stress induced calcium signalling of cells, achieved through varying the flow rate applied to the microfluidic platform (such as 120 μl/min). (iii) Investigating concurrent chemical and shear stress induced calcium signalling of cells. Scale Bar: 50 μm.

microelectrodes by applying an alternating-current sinusoidal signal operating at 10 MHz, 5 $V_{pk\text{-}pk}$ (see supplementary material S2 for corresponding electric field contours).[46] The electric field was deactivated after 120 s, which enables a suitable population of cells to be immobilised, and the LEC buffer was exchanged for HBS, following which HBS is washed through the microchannel for 10 min to enable cells to reach equilibrium. After this wash, the activating stimuli such as chemical (agonist) and shear stress were applied to the immobilised cells. The cells remain immobilised in flow rates of 180 μl/min (63 dyn/cm^2) using discontinuous dielectrophoresis with an efficiency greater than 90% (Figure 1(b)).[39] As we previously conjectured, we attributed this high trapping efficiency to an increase in the adhesion properties of the *cell adhesion molecules (CAMs)*, when invoking discontinuous dielectrophoresis.[39,47–49] Propidium iodide in HBS, at a flow rate of 2.5 μl/min, was used to assess cell viability at the conclusion of each experiment. As previously reported, discontinuous dielectrophoresis did not have adverse effects on cell viability. At the completion of the discontinuous dielectrophoresis procedure, a viability assay was completed for a 240 min duration, which presented with a viability of 90%.[39]

Stimulation mechanisms we investigated after carrying out discontinuous dielectrophoresis were chemical (pharmacological agonism), shear stress, and concurrent chemical and shear stress (Figure 1(b)). Chemical stimulation (Figure 1(b-i)) was achieved by adding a desirable concentration of a selected chemical into the inlet reservoir of the microfluidic platform. The selected chemical was applied with a low flow rate to the immobilised cells, thus producing a negligible shear stress of 0.875 dyn/cm^2. As an example of chemical (agonist) stimulation, HEK-293 cells expressing TRPV4 were stimulated with a TRPV4-selective agonist, GSK1016790A (prepared as explained in the "Materials and Methods" section). Shear stress stimulation (Figure 1(b-ii)) was achieved by increasing the flow rate, for example, to 120 μl/min to produce shear stress of 42 dyn/cm^2 over the immobilised cells. Concurrent chemical and shear stress stimulation (Figure 1(b-iii)) was achieved by applying the desired chemical (GSK1016790A, in our case) via the inlet reservoir of the microfluidic platform, whilst increasing the flow rate to induce the desired levels of shear stress over the immobilised cells.

Chemical stimulation: Agonist GSK1016790A

In brief, chemical stimulation is achieved by first carrying out discontinuous dielectrophoresis (Figure 1(a)), then applying the desired chemical to the microfluidic platform, which in our case was the agonist GSK1016790A. The chemical was supplied to the immobilised cells, by applying a low flow rate (2.5 μl/min)—which ensured that the shear stress experienced by the immobilised cells was negligible (0.875 dyn/cm^2) (Figure 1(b-i)).

An LEC suspension is commonly used for dielectrophoresis-based experiments and has been previously reported to affect the viability of cells over an extended duration.[50] Such reduction of viability can be attributed to the fact that LEC is absent of essential ions, such as calcium that assist in regulating biological functioning.[1,51] However, the influence of LEC on cell functioning in regards to intracellular calcium signalling has not been examined. To investigate this, we compared the agonist-induced calcium signalling of HEK-293-TRPV4 cells suspended in LEC in relation to those suspended in HBS. Two different concentrations of GSK1016790A of 3.125 and 12.5 nM were selected for the comparison experiments between the two buffers. As a negative control, we measured responses from non-transfected (NT) cells under the same concentrations of GSK1016790A. All experiments were conducted at a low flow rate of 2.5 μl/min (corresponding to a shear stress of 0.875 dyn/cm^2) to mitigate the impact of shear stress. GSK1016790A induced calcium influx was quantified by measuring the changes in the fluorescent intensity of the Fluo-4AM, which was normalised to the basal level over a duration of 600 s, with GSK1016790A being applied to the system at 60 s, as presented in Figures 2(a) and 2(b) (see supplementary material S3 for experimental fluorescent images).[46] In order to understand the influence of suspension medium on the characteristics of calcium influx, we compared four parameters (Figure 2(c)): (i) the cellular response time; (ii) the peak response time; (iii) the maximum fold increase of intracellular calcium level ($[Ca^{2+}]_i$, pharmacological efficacy; and (iv) the percentage of activated cells.

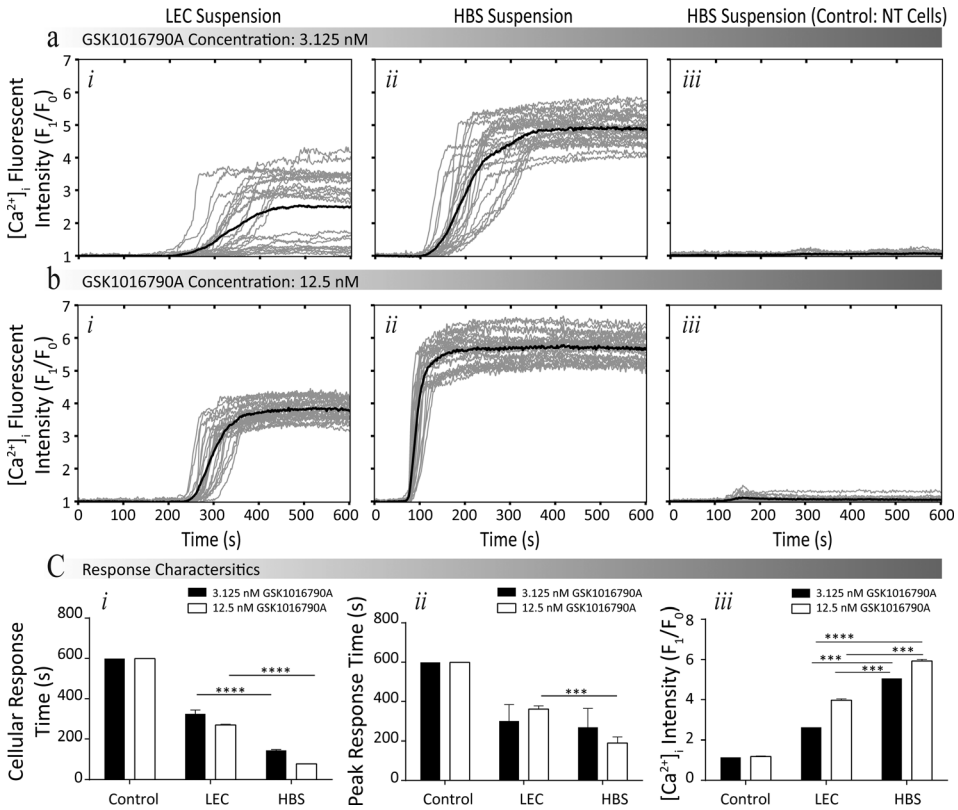

FIG. 2. Comparing the influence of LEC and HBS suspensions, in regard to the intracellular calcium signalling of HEK-293-TRPV4 cells. (a) and (b) Normalised intensity profiles at different concentrations of GSK1016790A (3.125 nM and 12.5 nM, respectively), conducted for HEK-293-TRPV4 cells suspended in (i) LEC, (ii) HEPES, and (iii) NT HEK-293 cells suspended in HEPES (Negative control) (see supplementary material S3 for experimental fluorescent images).[46] (c) Comparing the response characteristics: (i) cellular and (ii) peak response times, and (iii) pharmacological efficacy of cells suspended in different buffers. Data are presented as the mean ± SEM, ***$P < 0.001$, and ****$P < 0.0001$.

The cells suspended in HBS exhibited a faster rise in $[Ca^{2+}]_i$ than the cells suspended in LEC. For example, in the presence of 3.125 nM GSK1016790A, the cellular response time in HBS was 179 ± 11 s ($P < 0.001$, $N = 4$) shorter than cells in LEC. Additionally, the use of HBS reduced the peak response time. For example, in the presence of 12.5 nM GSK1016790A, the peak response time in HBS was 172 ± 25 s ($P < 0.001$, $N = 4$) shorter compared to the cells suspended in LEC. Additionally, the response characteristics indicated that increasing the concentration of GSK1016790A reduced the peak response time for cells suspended in HBS by 78 ± 24 s ($P < 0.05$, $N = 4$); however, no significant change was observed in LEC. Increasing the concentration of GSK1016790A from 3.125 to 12.5 nM caused an increase in the maximum fold increase of $[Ca^{2+}]_i$ regardless of the suspension medium. However, the cells suspended in HBS exhibited higher maximum responses (efficacy) compared to the cells suspended in LEC. At a GSK1016790A concentrations of 3.125 and 12.5 nM, a difference of 2.4 ± 0.2 ($P < 0.01$, $N = 4$) and 1.9 ± 0.2 ($P < 0.001$, $N = 4$) was observed, respectively. The percentage of activated HEK-293-TRPV4 cells in response to 3.125 nM GSK1016790A was 16 ± 1% fold ($N = 4$) higher in HBS, rather than LEC, with a smaller difference observed at higher concentrations of GSK1016790A. In addition, a negligible response was observed when using the control negative group (non-transfected HEK293 cells) in HBS, regardless of GSK1016790A concentration. The cells had a viability rate of 98.3 ± 0.6%, 99.2 ± 0.3%, and 98.9 ± 0.2% for the control, cells suspended in HBS and LEC, respectively. Thus, indicating the viability of cells was not influenced by the application of GSK1016790A or the buffer.

The intracellular Ca^{2+} signalling can arise from Ca^{2+} influx from external sources (such as a buffer) as well as Ca^{2+} release from intracellular stores. As such, buffers that modulate the

amplitude, duration, and extent of Ca^{2+} influx have a significant influence on intracellular Ca^{2+} signalling.[52] Furthermore, the measurement of changes in intracellular Ca^{2+} under the stage of microscope needs to be performed in an atmosphere containing a small concentration of carbon dioxide (usually 5%), undertaken in a specialised incubator to control the concentration of gas dissolved and maintain cell physiological conditions. HBS is commonly used in live cell microscopy to maintain pH levels in the absence of 5% carbon dioxide atmosphere.[53] In addition, the presence of sufficient amount of salts in HBS maintains the osmotic pressure of the cells.[54] The absence of any pH buffering component and physiological level of salts (for example, $CaCl_2$) in the LEC buffer interfere with Ca^{2+} signalling; this is due to LEC not maintaining the physiological conditions such as pH, osmotic pressure, as well as Ca^{2+} influx.

Shear stress simulation analysis

Discontinuous dielectrophoresis (Figure 1(a)) as discussed above enables cells to remain immobilised under high shear stress levels. An analysis of the effect of shear stress on immobilised cells was performed. The spherical shape of the cell was preserved, during and after immobilisation achieved using discontinuous dielectrophoresis. However, the immobilised cells alter the spatial distribution of flow variables, including the flow velocity and velocity gradients close to the cells. Consequently, these gradients cause a change in magnitude of the flow-induced shear stress, in comparison to the absence of cells. We present here, the simulation results to provide an insight into the shear stress experienced by immobilised cells in different configurations (Figures 3 and 4). Configurations investigated, include single, double, and triple cells patterned parallel or normal to the direction of flow. An extended cluster configuration, containing two rows with seven cells in each row was also investigated.

For the simulations, the diameter of cells was set to 15 μm the diameter of HEK-293 cells. Furthermore, the cells are pushed 1.5 μm towards the glass substrate to mimic the deformation of the cell, when immobilised on the glass substrate (see supplementary material S4).[46] The spherical structure above the glass surface is then scaled up accordingly to ensure the volume of a single cell is maintained. Similarly, for the case of adjacent cells, the cells are pushed 1.5 μm towards each other to mimic the local deformations, which occur at the interface of adjacent cells. The merged structure is scaled up accordingly to maintain the total volume of constituent cells (see supplementary material S5).[46]

During the application of high flow rates, the electric field is inactive (Figure 1); thus, the deformation of cells due to strong electric fields and the formation of secondary flows (such as electro-thermal vortices) due to Joule heating effects were not accounted for in our simulations. *Reference shear* is defined as the maximum shear stress experienced along the flat surface of a glass slide in the absence of immobilised cells. For the simulations, a flow rate of 120 μl/min was used, which corresponds to the highest flow rate reported in this paper used for investigating the response of cells to shear stress stimulus. The *reference shear* at the aforementioned flow rate is 42 dyn/cm^2 for a microfluidic channel with dimensions of 500 $\times$ 80 μm (see supplementary material S6).[46]

In the case of a *single cell* (Figure 3(a-i)), a maximum shear stress of 191 dyn/cm^2 (indicated in dark red) was obtained along the surface at the top of the cell, which is approximately 4.5 times greater than the magnitude of the *reference shear*. However, the cell surface regions in close proximity to the glass substrate experience the lowest shear stress ranging between zero and 29 dyn/cm^2, which corresponds to the low flow velocities experienced in these regions. Consequently, the average shear stress over the entire cell was determined to be 58 dyn/cm^2, which is approximately 1.4 times the magnitude of the *reference shear* (Figure 3(b)).

For the case of *double cells* patterned parallel to flow (Figure 3(a-ii)), the extent of the maximum shear stress region along the surface at the top of the cells was smaller compared to the case of single cell, especially for the back/downstream positioned cell that is located in the "shadow" of the front/upstream cell. Furthermore, the low shear stress is experienced close to the interface of the two cells. Consequently, the average shear stress of the front and back

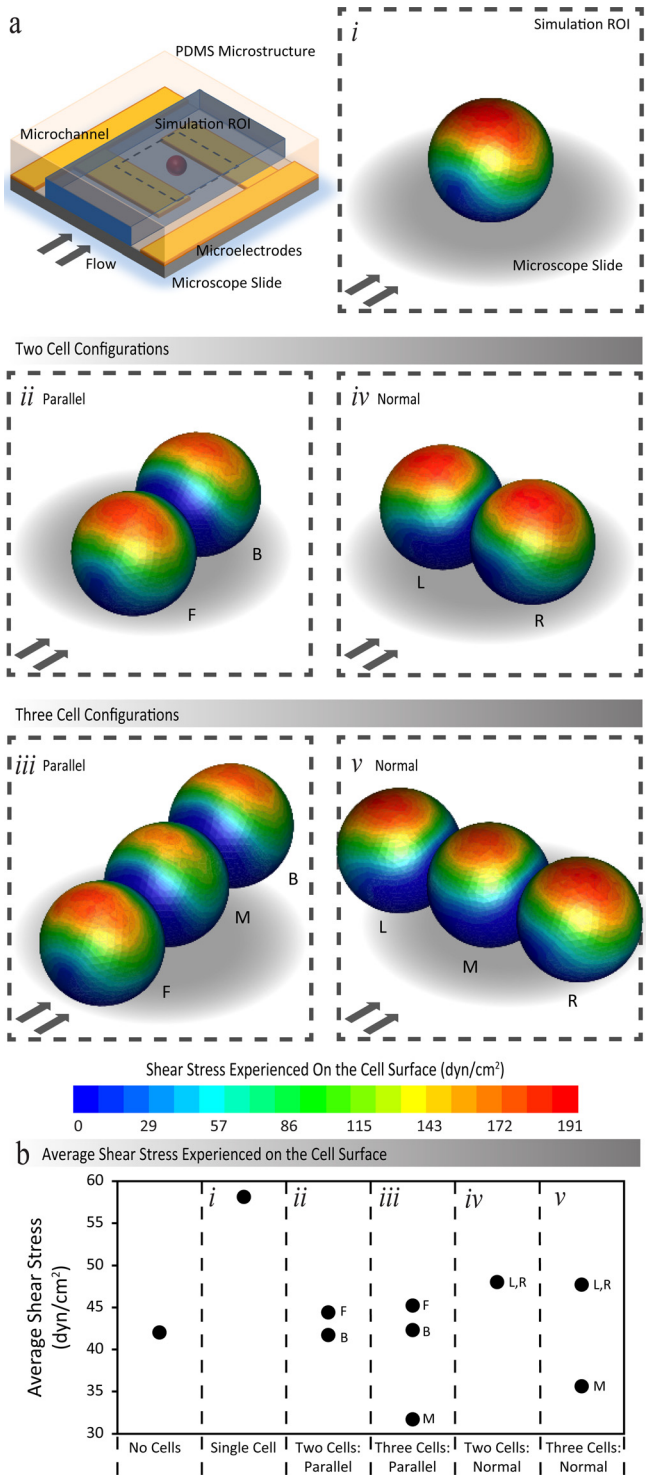

FIG. 3. (a) Contours of shear stress exerted over a cluster of immobilised HEK-293 cells, obtained through numerical stimulations when a flow rate of 120 μl/min is applied through the microchannel. The presented results display the shear stress experienced for a single cell, double and triple cells, patterned parallel and normal to the direction of flow. (b) The values of average shear stress exerted on cells in different configurations. F and B are used to denote the front and back positioned cells, and L, M, and R are used to denote the left, middle, and right positioned cells.

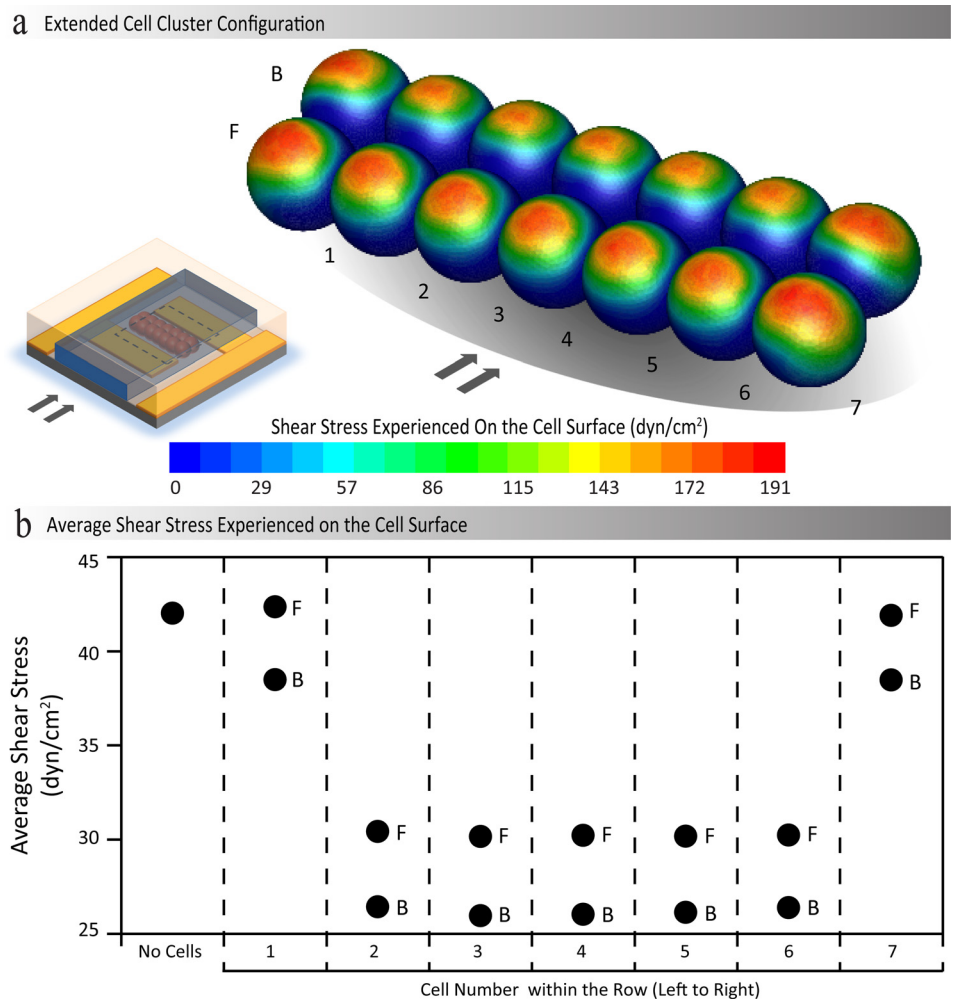

FIG. 4. (a) Contours of shear stress exerted over a cluster of immobilised HEK-293 cells, obtained through numerical stimulations when a flow rate of 120 μl/min is applied through the microchannel. (b) The values of average shear stress exerted on different cells within the cluster. F and B are used to denote the front and back rows of the cluster, respectively; in addition, 1 to 7 are used to denote the location of the cell in the row from left to right.

positioned cells was determined to be 44.4 and 41.7 dyn/cm^2, respectively—both are similar in magnitude to the *reference shear* (Figure 3(b)).

Similar patterns were observed for the case of *triple cells* patterned parallel to flow, as presented in Figure 3(a-iii). Interestingly, our simulations revealed that the middle cell experiences less shear compared to the front and back cells. This was attributed to the local distribution of flow velocity around a chain of cells, implying that the middle cell is located in the "shadow" of the first and last cells within the chain. The average shear stress levels experienced by the front and back positioned cells were calculated as 45.2 and 42.3 dyn/cm^2, respectively—both of which are similar to the *reference shear*. In contrast, the average shear over the middle cell was determined to be 31.7 dyn/cm^2—which is 0.8 times the magnitude of the *reference shear* (Figure 3(b)).

For the case of *double cells* patterned normal to flow, as presented in Figure 3(a-iv), the extent of the maximum shear stress regions is comparable to that of *single cell*. However, the shear stress reduced along the interface of the two adjacent cells, which can be readily observed in the back cell in Figure 3(a-iv). As a result, an average shear stress level of 48 dyn/cm^2 was determined for both cells—which is 1.1 times the magnitude of the *reference shear* (Figure 3(b)).

Similar patterns were observed for case of *triple cells* patterned normal to flow (Figure 3(a-v)). The low shear stress regions were observed along the interfaces of adjacent cells. The middle cell experiences a lower shear stress compared to the left and right cells, as evidenced by the extent of the red regions. This was attributed to the changes in the local distribution of the flow, as the flow tries to divert the cell cluster. Accordingly, an average shear stress level of 47.7 dyn/cm^2 was determined for the left and right cells—which is 1.1 times the magnitude of the *reference shear*. In comparison, the middle cell experiences an average shear stress of 35.6 dyn/cm^2, which is 0.9 times the magnitude of the *reference shear* (Figure 3(b)).

To further investigate the variations of shear stress over immobilised cell clusters, we simulated an extended cluster of 14 cells containing two rows with seven cells in each row (Figure 4(a)). This cluster provides a more detailed insight into the shear stress experienced by cells immobilised on the platform; due to the fact that multiple rows of cells of various widths form on the substrate, when using dielectrophoresis to immobilise the cells.

Our simulations indicated that the top surface of all the cells experience the highest shear stress, which is similar to the case of "single cell" presented in Figure 3(a-i). However, the extent of the maximum shear stress regions (indicated in red on the simulated cells) varies amongst different cells within the cluster, as observed in the prior analysis of single cell, double, and triple cells in both parallel and normal configurations (Figure 3). The prior analysis provided an insight into these variances, as follows. (i) In general, the shear stress is minimal along the interface of adjacent cells, and the cell surface regions close to the substrate (as can be identified by coverage of the blue regions). (ii) The cells located at the ends of the rows (designated with numbers 1 and 7) experienced a higher shear compared to the cells located in the middle of the rows. (iii) The cells located in the back row experienced a lower shear compared to the cells located within the front row. Such variations influence the average shear stress exerted on different cells within the cluster, as compared in Figure 4(b). The cells located at the ends of the rows experience an average shear stress ranging from 38.5 to 42.1 dyn/cm^2, which is comparable to the *reference shear*. In contrast, the cells located in the middle of the rows experience an average shear stress ranging from 25.9 to 30.2 dyn/cm^2, which is 0.6 to 0.7 times the magnitude of the *reference shear*. The overall average shear stress of the cell cluster was determined to be 31.7 dyn/cm^2, which is 0.8 times the magnitude of the *reference shear*. Similar trends were obtained when the second row of cells is patterned with a lateral offset with respect to the first row (see supplementary material S7).[46] Interestingly, in this case, the average shear stress is 5%–8% higher compared to the case of no offset, which was explored above. Thus, we use the *reference shear* as a sufficient approximation of the shear stress experienced by immobilised cells within the microchannel, primarily due to the variability of the configuration of the patterned cell clusters when immobilising cells using dielectrophoresis.

Concurrent chemical and shear stress stimulation

In brief, concurrent chemical and shear stress stimulation was achieved by first carrying out discontinuous dielectrophoresis (Figure 1(a)), then concurrently applying the desired chemical (agonist, GSK1016790A) to the microfluidic platform as the flow rate was increased (Figure 1(b-iii)). Discontinuous dielectrophoresis enabled the immobilised cell clusters to withstand high levels of shear stress with a trapping efficiency greater than 90% at a flow rate of 180 μl/min.[39] The trapping efficiency was not influenced by the presence of GSK1016790A. The preceding "Shear stress simulation analysis" section provided an insight into the shear stress experienced by HEK-293 cells immobilised within the microfluidic channel. Taking note the level of shear stress experienced on the cells is denoted with the *reference shear*, as previously explained why using the reference shear is a suitable approximation for the shear stress experienced by the immobilised cells. This section examines the characteristics of HEK-293-TRPV4 intracellular calcium levels in response to shear stress in both the absence and presence of chemical stimulation.

To examine the intracellular calcium signalling of HEK-293-TRPV4 under concurrent shear stress and chemical stimuli, we conducted experiments at three different flow rates of 2.5, 30, and 120 μl/min corresponding to *reference shear* values of 0.875, 10.5, and 42 dyn/cm^2.

Experiments were conducted using the experimental procedure outlined in Figure 1(b-iii) for cells suspended in HBS (see supplementary material S6 for velocity and shear stress profiles).[46] At each *reference shear*, we examined three different concentrations of GSK1016790A being 0.0 (control, no GSK1016790A), 3.125, and 12.5 nM. Concurrent shear stress and GSK1016790A induced calcium influx were quantified by measuring the changes in the intensity of the Fluo-4AM normalised to the basal level over the experimental duration of 900 s, with stimulus being applied at 60 s, as presented in Figures 5(a)–5(c) (see supplementary material S8 for experimental fluorescent images).[46] In order to understand the influence of these stimuli on the characteristics of calcium influx, we compared four parameters (Figure 5(d)): (i) the cellular response time; (ii) the peak response time; (iii) the maximum fold increase of $[Ca^{2+}]_i$, pharmacological efficacy; and (iv) the percentage of activated cells. The viability was determined to be $98 \pm 1\%$ across the experiments with no significant difference observed at different chemical concentrations and shear stress levels (supplementary material S8).[46]

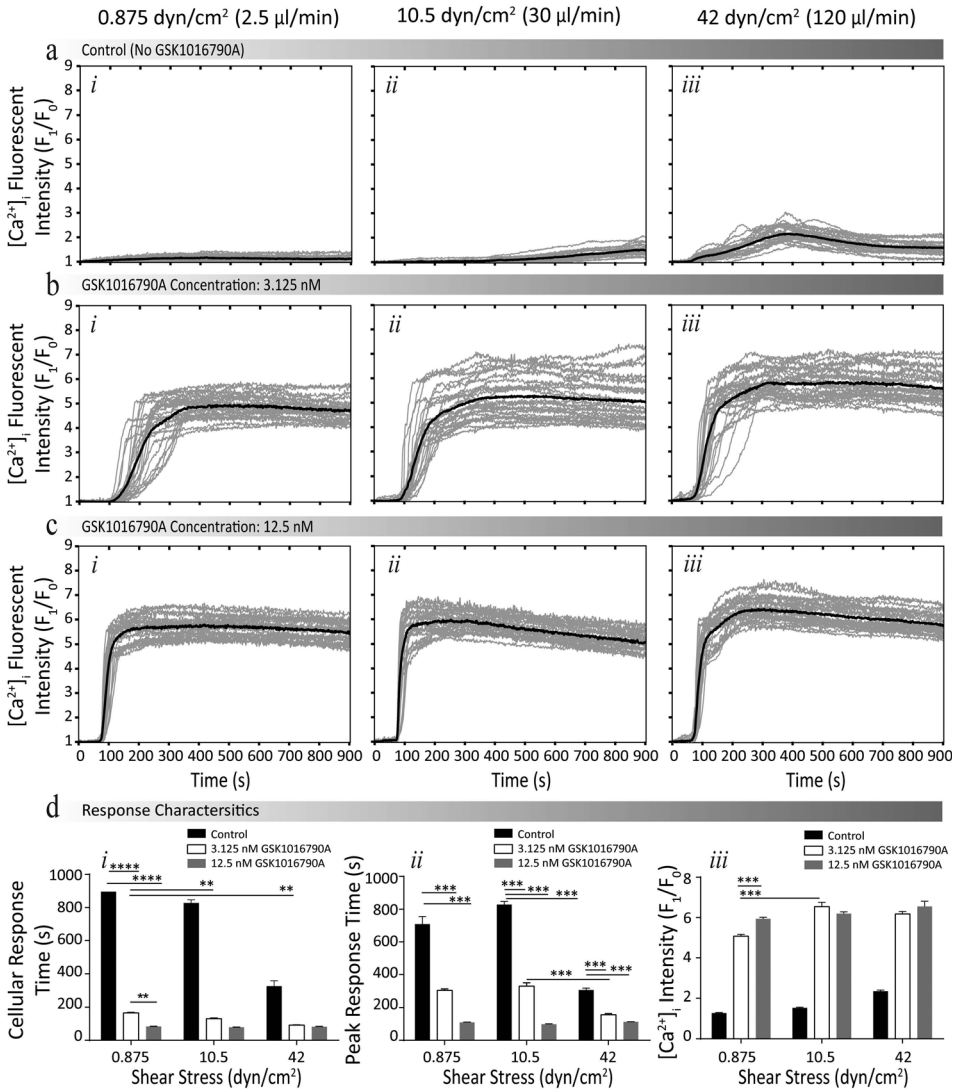

FIG. 5. Intracellular calcium signalling response of HEK-293-TRPV4 cells under concurrent shear stress and GSK1016790A stimulation. (a)–(c) Normalised intensity profiles at different concentrations of GSK1016790A (control (0.0 nM), 3.125 nM, and 12.5 nM, respectively), obtained at the *reference shear* values of (i) 0.875, (ii) 12.5, and (iii) 42 dyn/cm^2 (see supplementary material S8 for experimental fluorescent images).[46] (d) Comparing the response characteristics: (i) cellular and (ii) peak response times, and (iii) pharmacological efficacy of cells under different shear stress levels. Data are presented as the mean ± SEM, *P < 0.05, **P < 0.01, ***P < 0.001, and ****P < 0.0001.

A reduction in the cellular response time was observed with an increase in shear stress regardless of the concentration of GSK1016790A. For example, in the presence of 3.125 nM GSK1016790A, increasing shear stress from 0.875 to 10.5 dyn/cm^2 reduced the cellular response time by 35 ± 19 s ($P < 0.001$, $N = 4$). Furthermore, no general trend was observed in the peak response time with an increase of shear stress. However, with an increase in GSK1016790A at each shear stress level, a reduction in the peak response time was observed. For example, increasing the concentration of GSK1016790A from 3.125 to 12.5 nM reduced the peak response time by 194 ± 27 s ($P < 0.01$, $N = 4$) at the shear stress level of 0.875 dyn/cm^2. Additionally, we observed an increase in the pharmacological efficacy, when a higher shear stress was applied, regardless of the concentration of GSK1016790A. For example, in the presence of 3.125 nM GSK1016790A, an increase of shear from 0.875 to 10.5 dyn/cm^2 increased the $[Ca^{2+}]_i$ by 1.28 ± 0.17 fold ($P > 0.001$, $N = 4$); or in the presence of 12.5 nM GSK1016790A, an increase of shear from 10.5 to 42 dyn/cm^2 increased the $[Ca^{2+}]_i$ by 0.7 ± 0.2 fold ($P > 0.001$, $N = 4$). With an increase in shear stress, in the presence of GSK1016790A, no clear influence in the percentage of activated cells was observed, potentially due to the Ca^{2+} response becoming saturated. However, in the absence of GSK1016790A, elevating the shear stress level from 10.5 to 42 dyn/cm^2 increased the percentage of activated cells by $59 \pm 1\%$ fold ($N = 4$).

Our experiments indicated that the GSK1016790A induced calcium signalling of cells can be greatly affected by the shear stress. We observed similar responses for vascular endothelial cells due to an increase in plasma membrane density of TRPV4 channels. The data presented here are consistent with our previous discovery that the shear stress induces exocytosis of functional TRPV4 channels to the plasma membrane of vascular endothelial cells to sensitise TRPV4.[55] Consequently, confirming that discontinuous dielectrophoresis did not prevent the functional properties of cell responses to chemical and mechanical activators of TRPV4.

CONCLUSIONS

Here, we have demonstrated through experiments and statistical analysis the effect of mechanical stimulation on agonist activation in HEK-293-TRPV4 cells. The immobilisation of the loosely adherent cells was achieved through the use of the discontinuous dielectrophoresis procedure, which enabled high shear stress analysis to be undertaken. Concurrently, we stimulated cells with the TRPV4-selective agonist GSK1016790A and shear stress. Experiments were conducted at different agonist concentrations and shear stress levels (through applying an appropriate flow rate). Taking note that high shear stress of 42 dyn/cm^2 was achieved in the presence of chemicals (GSK1016790A) with the loosely adherent cells (HEK-293-TRPV4) remaining immobilised to the glass substrate of the platform.

Our experiments revealed that the calcium signalling of cells is influenced by the buffer, as observed through comparing cellular and peak response times, percentage of activated cells, for cells suspended in HEPES and LEC buffers. Additionally, our experiments revealed that the shear stress sensitises GSK1016790A-evoked intracellular calcium signalling of cells in a shear-stimulus dependent manner; thus, suggesting that the role of TRPV4 may be underestimated in endothelial cells, which experience high levels of shear stress.

The microfluidic system described facilitated the investigation of intracellular calcium signalling of cells that do not attach well to surface, or, which are normally grown in suspension. Experiments can be conducted under various combinations of concurrent chemical and physical stimuli with an emphasis of high shear stress stimulation. Additionally, the microfluidic platform enables dynamic control, such that the concentration or even composition of chemicals can be modified on demand, or, that the shear stress can be changed dynamically to mimic physiological conditions.

ACKNOWLEDGMENTS

Khashayar Khoshmanesh acknowledges the Australian Research Council for funding, under the Discovery Early Career Researcher Award (DECRA) scheme (Project No. DE120101402).

[1]E. Carafoli, Annu. Rev. Biochem. **56**(1), 395–433 (1987).
[2]J. El-Ali, P. K. Sorger, and K. F. Jensen, Nature **442**(7101), 403–411 (2006).
[3]S. Nahavandi, S.-Y. Tang, S. Baratchi, R. Soffe, S. Nahavandi, K. Kalantar-zadeh, A. Mitchell, and K. Khoshmanesh, Small **10**(23), 4810–4826 (2014).
[4]W. J. Polacheck, R. Li, S. G. Uzel, and R. D. Kamm, Lab Chip **13**(12), 2252–2267 (2013).
[5]G. Bao and S. Suresh, Nat. Mater. **2**(11), 715–725 (2003).
[6]X. Mu, W. Zheng, J. Sun, W. Zhang, and X. Jiang, Small **9**(1), 9–21 (2013).
[7]R. Soffe, S.-Y. Tang, S. Baratchi, S. Nahavandi, M. Nasabi, J. M. Cooper, A. Mitchell, and K. Khoshmanesh, Anal. Chem. **87**(4), 2389–2395 (2015).
[8]S.-Y. Tang, P. Yi, R. Soffe, S. Nahavandi, R. Shukla, and K. Khoshmanesh, Anal. Bioanal. Chem. **407**(12), 3437–3448 (2015).
[9]J. Guck, F. Lautenschläger, S. Paschke, and M. Beil, Integr. Biol. **2**(11–12), 575–583 (2010).
[10]A. Pavesi, G. Adriani, M. Rasponi, I. K. Zervantonakis, G. B. Fiore, and R. D. Kamm, Sci. Rep. **5**, 11800 (2015).
[11]N. M. Alves, I. Pashkuleva, R. L. Reis, and J. F. Mano, Small **6**(20), 2208–2220 (2010).
[12]J. L. Prieto, J. Lu, J. L. Nourse, L. A. Flanagan, and A. P. Lee, Lab Chip **12**(12), 2182–2189 (2012).
[13]J.-R. Choi, H. Song, J. H. Sung, D. Kim, and K. Kim, Biosens. Bioelectron. **77**, 227–236 (2016).
[14]J. R. Choi, R. Tang, S. Wang, W. A. B. Wan Abas, B. Pingguan-Murphy, and F. Xu, Biosens. Bioelectron. **74**, 427–439 (2015).
[15]S. H. Lee, E. H. Oh, and T. H. Park, Biosens. Bioelectron. **74**, 554–561 (2015).
[16]C. Szydzik, K. Khoshmanesh, A. Mitchell, and C. Karnutsch, Biomicrofluidics **9**(6), 064120 (2015).
[17]C. Huang, J. P. Smith, T. N. Saha, A. D. Rhim, and B. J. Kirby, Biomicrofluidics **8**(4), 044107 (2014).
[18]R. Pethig, Biomicrofluidics **4**(2), 022811–022835 (2010).
[19]D. Holmes, N. G. Green, and F. Morgan, IEEE Eng. Med. Biol. **22**(6), 85–90 (2003).
[20]L. Y. Yeo, H.-C. Chang, P. P. Y. Chan, and J. R. Friend, Small **7**(1), 12–48 (2011).
[21]P. F. Neill, A. Ben Azouz, M. Vázquez, J. Liu, S. Marczak, Z. Slouka, H. C. Chang, D. Diamond, and D. Brabazon, Biomicrofluidics **8**(5), 052112 (2014).
[22]M. Junkin, Y. Lu, J. Long, P. A. Deymier, J. B. Hoying, and P. K. Wong, Biomaterials **34**(8), 2049–2056 (2013).
[23]P. Chen, P. Chen, X. Feng, W. Du, and B.-F. Liu, Anal. Bioanal. Chem. **405**(1), 307–314 (2013).
[24]X. Li, J. Huang, G. F. Tibbits, and P. C. Li, Electrophoresis **28**(24), 4723–4733 (2007).
[25]F. Guo, J. B. French, P. Li, H. Zhao, C. Y. Chan, J. R. Fick, S. J. Benkovic, and T. J. Huang, Lab Chip **13**(16), 3152–3162 (2013).
[26]S. L. Faley, M. Copland, D. Wlodkowic, W. Kolch, K. T. Seale, J. P. Wikswo, and J. M. Cooper, Lab Chip **9**(18), 2659–2664 (2009).
[27]T. Xu, C.-W. Li, X. Yao, G. Cai, and M. Yang, Anal. Biochem. **396**(2), 173–179 (2010).
[28]K. Chung, C. A. Rivet, M. L. Kemp, and H. Lu, Anal. Chem. **83**(18), 7044–7052 (2011).
[29]M. Kato and M. Mrksich, J. Am. Chem. Soc. **126**(21), 6504–6505 (2004).
[30]C. S. Simmons, J. Y. Sim, P. Baechtold, A. Gonzalez, C. Chung, N. Borghi, and B. L. Pruitt, J. Micromech. Microeng. **21**(5), 54016–54025 (2011).
[31]K. Yamamoto and J. Ando, J. Cell Sci. **126**(5), 1227–1234 (2013).
[32]S. Baratchi, F. J. Tovar-Lopez, K. Khoshmanesh, M. S. Grace, W. Darby, J. Almazi, A. Mitchell, and P. McIntyre, Biomicrofluidics **8**(4), 044117(044111–044113) (2014).
[33]W. Cheng, N. Klauke, G. Smith, and J. M. Cooper, Electrophoresis **31**(8), 1405–1413 (2010).
[34]T. Xu, W. Yue, C.-W. Li, X. Yao, and M. Yang, Lab Chip **13**(6), 1060–1069 (2013).
[35]J. Voldman, Curr. Opin. Biotechnol. **17**(5), 532–537 (2006).
[36]I. Mutreja, T. B. F. Woodfield, S. Sperling, V. Nock, J. J. Evans, and M. M. Alkaisi, Biofabrication **7**(2), 025002 (2015).
[37]S. A. Mendoza, J. Fang, D. D. Gutterman, D. A. Wilcox, A. H. Bubolz, R. Li, M. Suzuki, and D. X. Zhang, Am. J. Physiol.: Heart Circ. Physiol. **298**(2), H466–H476 (2010).
[38]H. Kaji, M. Kanada, D. Oyamatsu, T. Matsue, and M. Nishizawa, Langmuir **20**(1), 16–19 (2003).
[39]R. Soffe, S. Baratchi, S.-Y. Tang, M. Nasabi, P. McIntyre, A. Mitchell, and K. Khoshmanesh, Sci. Rep. **5**, 11973; doi:10.1038/srep11973 (2015).
[40]D. N. Ku, D. P. Giddens, C. K. Zarins, and S. Glagov, Arterioscler., Thromb., Vasc. Biol. **5**(3), 293–302 (1985).
[41]D. E. Jaalouk and J. Lammerding, Nat. Rev. Mol. Cell Biol. **10**(1), 63–73 (2009).
[42]G. P. Ahern, Trends Endocrinol. Metab. **24**(11), 554–560 (2013).
[43]D. P. Poole, S. Amadesi, N. A. Veldhuis, F. C. Abogadie, T. Lieu, W. Darby, W. Liedtke, M. J. Lew, P. McIntyre, and N. W. Bunnett, J. Biol. Chem. **288**(8), 5790–5802 (2013).
[44]F. Vincent and M. AJ Duncton, Curr. Top. Med. Chem. **11**(17), 2216–2226 (2011).
[45]G. M. Whitesides, E. Ostuni, S. Takayama, X. Jiang, and D. E. Ingber, Annu. Rev. Biomed. Eng. **3**(1), 335–373 (2001).
[46]See supplementary material at http://dx.doi.org/10.1063/1.4945309 for a detailed description on: Microfluidic Platform Configuration and Design (S1); Electric Field Contours (S2); Effect of suspension media on the intracellular calcium signalling of HEK-293-TRPV4 cells (S3); Single Cell Simulation Structure (S4); Adjacent Cell Simulation Structure (S5); Velocity and Shear Stress Profiles (120 μl/min) (S6); Extended Cell Cluster Simulation Comparison (S7); and Intracellular calcium signalling of HEK-293-TRPV4 cells under concurrent shear stress and GSK1016790A stimulation (S8).
[47]H. F. Lodish, A. Berk, S. L. Zipursky, P. Matsudaira, D. Baltimore, and J. Darnell, *Molecular Cell Biology* (Citeseer, 2000).
[48]S. M. Albelda and C. A. Buck, FASEB J. **4**(11), 2868–2880 (1990).
[49]K. Zhang and J. Chen, Cell Adhes. Migr. **6**(1), 20–29 (2012).
[50]J. Voldman, Annu. Rev. Biomed. Eng. **8**, 425–454 (2006).
[51]K. Khoshmanesh, J. Akagi, S. Nahavandi, J. Skommer, S. Baratchi, J. M. Cooper, K. Kalantar-Zadeh, D. E. Williams, and D. Wlodkowic, Anal. Chem. **83**(6), 2133–2144 (2011).

[52]B. Nilius, J. Vriens, J. Prenen, G. Droogmans, and T. Voets, Am. J. Physiol.: Cell Physiol. **286**(2), C195–C205 (2004).
[53]A. Ettinger and T. Wittmann, Method Cell Biol. **123**, 77 (2014).
[54]F. R. Ian, *Culture of Animal Cells: A Manual of Basic Technique and Specialized Applications*, 6th ed. (Wiley-Sons, New York, 2010).
[55]S. Baratchi, J. G. Almazi, W. Darby, F. J. Tovar-Lopez, A. Mitchell, and P. McIntyre, Cell. Mol. Life Sci. **73**(3), 649–666 (2016).